


Stress intensity factors for micro-crack emanating from micro-cavity in cement of reconstructed acetabulum

N. Bounoua*, **A. Belarbi****, **M. Belhouari***, **B. Bachir Bouiadjra***

*LMPM, Department of Mechanical Engineering, University of Sidi Bel Abbes, BP 89, Cité Ben M'hidi, Sidi Bel Abbes 22000, Algeria, E-mail: nbounoua@yahoo.fr

**LASP, Department of Mechanical Engineering, USTMB, BP 1055 El Menaour, Oran, Algeria, E-mail: belarbi_abd@yahoo.fr

 <http://dx.doi.org/10.5755/j01.mech.20.6.9157>

1. Introduction

Different studies have investigated the influence of porosity on fatigue of cement [1-5]. Pores are of course significant stress concentration sites, readily initiating fatigue cracks [6-7]. The number and distribution of pores within the cement volume can have a significant effect on fatigue cracking; Hoey and Taylor [4] found crack initiation sites usually contained two or more pores in a cluster, while Murphy and Prendergast [8] reported crack initiation in the region of stress concentration between two pores. In vitro testing has demonstrated that a reduction in porosity corresponds to an increase in fatigue life [8-9]. Indeed, the negative influence of porosity on the mechanical performance of the cement in vitro led to the development of reduced pressure, vacuum-mixing methods in an attempt to minimize pore formation during clinical application [10-11]. While the relationship between porosity and fatigue life of cement in vitro is well established, in vivo results remain controversial. Ling and Lee [12] compared the survivorship of hip replacements with different cement porosities and concluded that the porosity reduction is clinically irrelevant. Murphy and Prendergast [8] are shown that the variability in porosity and the tendency for fewer, larger pores to be present in vacuum mixed cement, which are likely to cause significant stress concentrations, may explain the propensity for early failure in some cases. Thus, the mechanical and physical properties of cement are determining in the service life of the implant [13]. These properties are strongly affected by the size and number of pores in cement. Indeed, the porosity can cause crack initiation by fatigue, by creating irregular areas [14-15].

The presence of defect in the cement during mixing can locally lead to a region of stress concentrations producing a possible fracture of cement and consequently the loosening of the prosthetic cup. Almost there are three kinds of defects:

- porosities and micro cavities;
- inclusions;
- cracks.

It is known that cracks were the most dangerous defect because of the presence of stress intensity on their front. The most kinds of cracks observed in orthopedic cement are [16-17]:

- cracks initiated at porosities;
- cracks initiated during cement withdraw;
- cracks initiated at the junction between bone and cement or between cement and cup.

In the cemented femoral prosthesis, the structural strength of the total hip is provided by the cement, which Achour et al. [18] and Flitti et al. [19] presented that the mixed-mode crack propagation and the single-mode crack opening growth occur at the distal and proximal zones of the cement layer, respectively. The effect of the position and orientation of a crack in the cement in three loads using the finite element method has been studied by Serier et al. [20] and Bachir Bouiadjra et al. [21]. They indicate that, for the third case load, the risk of crack propagation is higher when the crack is in the horizontal position for both failure modes. The majority of previous studies were performed using a two-dimensional (2D) crack analysis by the standard finite element method (FEM). Oshkour et al. used the extended finite element method (XFEM) to simulate the internal circumferential cracks within the cement layer to analyze the SIFs variations in different cross sections (hoop direction) throughout the cement mantle length (longitudinal direction). Bouziane et al. [22] examined the behavior of micro-cavities located in the cement of a model of the hip prosthesis simplified three-dimensional. They show that when the micro-cavity is located at the proximal and distal areas, the static charge causes a higher stress field than the dynamic load. Benbarak et al. [23] shown that the variation of the stress intensity factors in mode I and II as a function of the length of the crack emanating from the micro-cavity and for a plurality of positions in the cement.

In this work, a three-dimensional finite element method was employed to analyze the behavior of the micro-crack emanating from a micro-cavity in acetabular cement mantle. The effect of axial and radial displacement of the micro-cavity in the cement is highlighted. To provide the place of birth of the micro-crack, the stress distribution around the micro-cavity is determined in several positions for different loading directions. Orthopedic cement is classified as a brittle material. Therefore, micro-crack analysis can be performed through linear elastic fracture mechanics.

2. Model definition

2.1. Geometrical and material model

Fig. 1 presents the geometrical model of the reconstructed acetabulum. The UHMWPE cup has an outer diameter of 54 mm and an inner diameter of 28 mm. It is sealed with the bone cement mantle to uniform thickness of 2 mm [24-26]. The interfaces between the cup-cement and cement-subchondral bone are assumed to be fully

bonded. The femoral head was modeled as a spherical surface that was attached to the spherical acetabular micro-cavity. The acetabular micro-cavity is located on the outside of the hip bone. This study aimed to investigate two case: the first is to take the presence of a micro-cavity in different positions within the cement layer. The stress concentrations are determined. The second case aimed to simulate the behavior of micro-crack emanating from the micro-cavity in the determined position and characterized by a high stress concentration gradient. The FEM was employed to identify the micro-crack behavior by studying various SIFs, that is, tensile, sliding, and tearing, which are denoted by K_I , K_{II} and K_{III} , respectively, at different heights during the main phases of the gait cycle. Semi-elliptical micro-crack emanating from micro-cavity with 0.2 mm of diameter is assumed to exist in the cement mantle. The dimensions of the micro-cracks are selected as follows: large half axis (length of the micro-crack) $c = 20.5 \mu\text{m}$, small half axis (depth of the micro-crack) $a = 8.5 \mu\text{m}$.

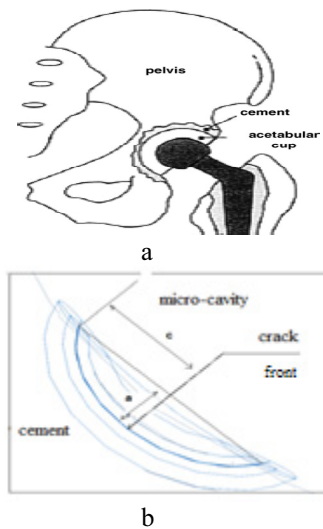


Fig. 1 Schematic of: a - reconstructed acetabulum; b - micro-crack position

The materials of cup, cement, bone layers and implant were defined as isotropic and linearly elastic. This is a reasonable assumption since the stresses are not enough high to create a plastic deformation of the polyethylene. Table 1 gives the elastic properties of the three materials: of prosthetic cup, cement, bone and implant [27, 28].

Table 1

Material properties

Materials	Young modulus E , MPa	Poisson ratio ν
Cortical bone	17000	0.30
Spongious bone	70	0.20
Cup (UHMWPE)	690	0.30
Cement (PMMA)	2000	0.30
Implant	210000	0.30

2.2. Loading model

The loading conditions depend on the activity of the hip joints. In fact, the kinematics of hip joints is quite

complicated and difficult to describe in a mathematical way. From gait analyses, it can be observed that the main activities of the foot are flexible and extendable in the walking direction, while other activities, such as abduction/adduction and femoral rotation, are negligible [29]. Consequently, we only need to simulate the activity of flexion and extension of the foot during the normal gait. For actual walking activities, each gait consists of two phases: standing and swing phases. Therefore, forces acting on hip joints are varied in magnitude with time during the gait period and can be referred to a dynamic loading. Saikko [30] measured the load history for each gait cycle by a five station hip joint simulator and declared the maximum force is 3.5 kN and the swing angle is 23° in the forward and backward directions for flexion/extension actions for each gait [29, 31]. Wu et al. [32] have divided Saikko's gait cycle into 16 load stages and the force acting on the hip joint for each stage may be obtained (Fig. 2).

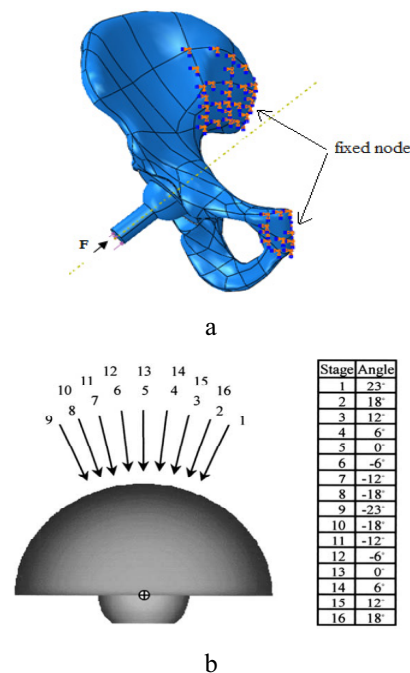


Fig. 2 Loading conditions: a - loading and boundary conditions; b - Forces acting on the hip joint in one gait cycle

The direction of the force applied to the hip joint model depends on the swing direction of the femoral head. Fig. 3, shows the amplitude of these forces applied to the artificial hip joint. Thus, the loading pressure imposed on the model for each stage is calculated from the magnitude of the force obtained and the projected area of the outer surface of compact bone normal to the direction of the

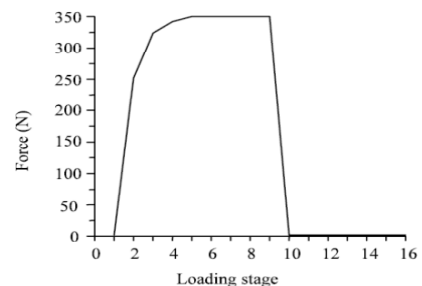


Fig. 3 Load amplitude for 16 stages in on gait cycle

force. The magnitude of forces applied to the artificial hip joint in every stage of each gait cycle can thus lead to the real contact status.

2.3. Finite element model

Computational methods such as finite element method are widely accepted in orthopedic biomechanics as an important tool used to design and analysis the mechanical behavior of prosthesis [33]. Several authors used this method to analyze the mechanical behavior of hip prosthesis. Contributing to this field, we analyzed the behavior of micro-cracks emanating from micro cavities in the cement layer, which fixes the acetabular cup to the contiguous bon, by calculating the stress intensity factor along the micro-crack front. The acetabulum was modeled using finite element code Abaqus [34]. Because of the interesting of the stress distribution around the micro cavities. A very high descritization were used with an advancing front meshing strategy to represent as possible the reality, and a focused mesh was used near a micro-crack tip. Two different cases were considered in the positioning of the micro-cavity and assessment of micro-crack behavior inside the cement layer. The first case was to locate the position of the micro-cavity in the cement layer to study the risky location in the cement with the highest stress concentrations. The second case was to examine the SIFs behaviors a along the micro-crack front. The micro-cavity was placed in the middle of the cement layer. In addition, different contours were considered to derive the SIFs.

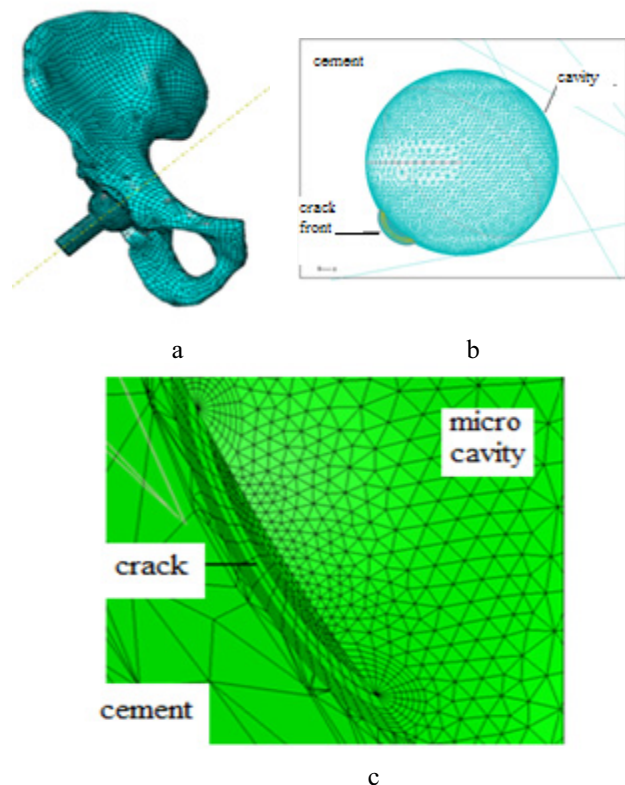


Fig. 4 Three-dimensional finite element mesh model: a. of the reconstructed acetabulum; b. near the micro-cavity and micro-crack tip; c. transverse section in the plane of the micro-crack

The computed SIFs in the different contours were compared with one another to check the accuracy and contour independency of the SIFs. The computed SIFs were determined to be close and independent of the selected contour. The stress intensity factor is computed using the modified micro-crack closure technique. The direct linear resolution was used to solve the stiffness matrix.

A 3D brick element with 8 nodes was used to mesh all models. The assembled model comprised 100528 elements (Fig. 4). A special mesh refinement is used near the micro-crack front with an aim of increasing the precision of calculations. A convergence test was conducted to achieve mesh indecency and to ensure model accuracy.

3. Analysis and results

3.1. Analyses of stresses in the cement layer

Before analyzing the stress intensity factor at the micro-crack tip, it was considered useful to determine the stress distribution around the micro-cavity in the cement layer without presence of micro-crack in order to analyze the nature of stresses in each position of cement and predict the micro-crack initiation location.

In this study two displacement of the micro-cavity were considered in order to locate the zones of stress concentration which are usually the sources of micro-crack initiation. In the first the micro-cavity is displaced in the angular direction from $\theta = 0$ to 90° (Fig. 5). The second case concerns the radial displacement of the micro-cavity.

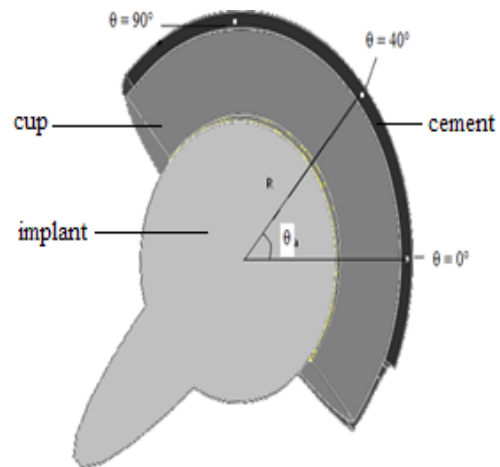


Fig. 5 Micro-cavity positions

3.1.1. Effect of angular displacement

Fig. 6 illustrate the distributions of the Von Misses equivalent stresses for different angular position of the micro-cavity ($R = 28$ mm). It can be seen that the stress distribution in the cement layer was not uniform around the micro-cavity. The extreme positions 0 and 90° generate almost the same distribution and the same level of stress. At these positions the maximum value of equivalent stress does not exceed 0.5 MPa. The Von Misses stresses increase with angle θ , where they reach their maximum values ($\sigma_{eq\ max} = 1.83$ MPa) at $\theta = 40^\circ$. Indeed, this position of the micro-cavity coincides with the femoral stem axis where the loading is applied. From $\theta = 40^\circ$, the intensity of

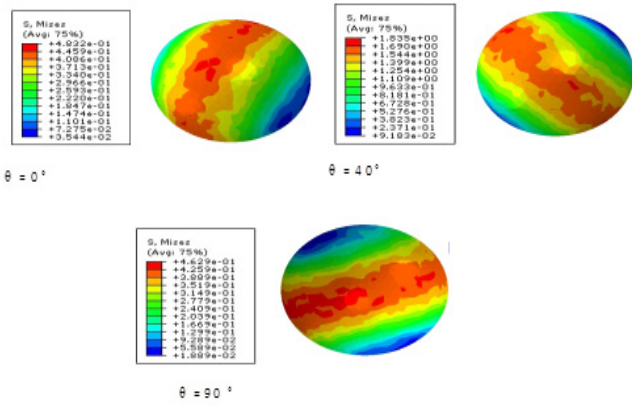


Fig. 6 Distributions of the Von Mises equivalent stresses in the cement mantle around micro-cavity for different angular position

equivalent stress decrease and reach their minimum value at 90°. It is also noted that the cement for different positions is subjected to tensile stress, this shows that the presence of micro-cavity in different regions can leads the fracture of the cement. Knowing that cement, in general do not resist to tensile loading well (tensile strength = 25 MPa, compressive strength = 80 MPa and the shearing strength = 40 MPa).

Fig. 7 illustrates the variations of maximum equivalent stress as a function of the position of the micro-cavity in cement layer. It can be noted that the position $\theta = 0$, instead of negligible stresses, the cement is completely relaxed. These stresses increase in intensity and reach their values maximum at $\theta = 40^\circ$. By symmetry these stresses decrease and reach their minimum values for $\theta = 90^\circ$. However, the stresses are extremely low they do not constitute an immediate risk of damage of the cement. But at the long term, these constraints can lead to failure of the cement. The cement around the micro-cavity is subjected to raise tensile loading.

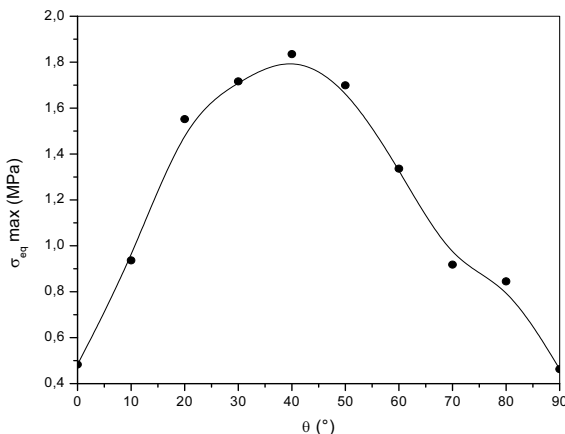


Fig. 7 $\sigma_{eq max}$ in the different position of the micro-cavity

This can constitute a major risk for the micro-crack initiation emanating from the micro-cavity, given that cement does not resist to the traction loading well.

3.1.2. Effect of radial displacement

This effect is shown in Fig. 8. This one presents the contour of the equivalent Von Mises stresses around

the micro-cavity moved along the radius R at position $\theta = 40^\circ$. This displacement is performed in the vicinity to the cement /cortical bone interface.

The radial displacement results an almost uniform distribution of stresses with the highest values is located in close vicinity of interface cup / cement. This can be mainly due to interaction effect between micro-cavity and cup with high mechanical properties. These stresses decrease intensity in the cement layer, where they reach their minimum value in the vicinity of the cement/cortical bone interface because to low mechanical properties of the bone.

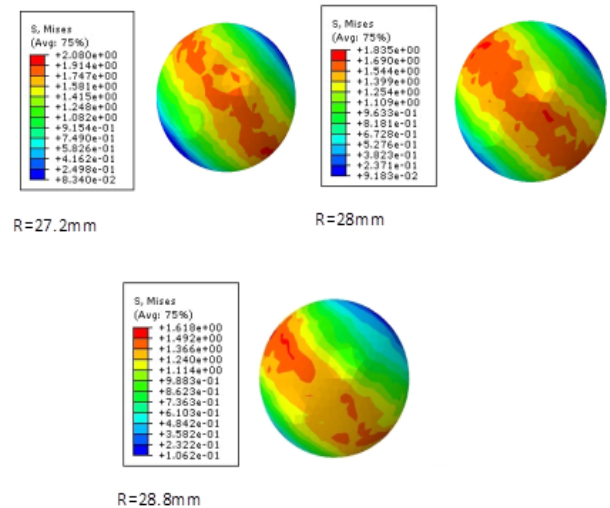


Fig. 8 Equivalent Von Mises stresses around micro-cavity for different radius R

The maximum stress at the interface cup-cement exceeds that at the bone-cement interface about 23%. The difference observed between maximum stresses, far and near vicinity of the interface, may be due to the interaction effect of stress field around the micro-cavity and interface.

The difference between the mechanical properties of assembled materials, characterized by the mechanical properties, determines the process of interaction effect. Bouziane et al. [22] examined the behavior of micro-cavity located in the cement of a model of the hip prosthesis simplified three-dimensional. They show that when the micro-cavity is located at the proximal part presents the most important risk of the rupture of the cement mantle; the interaction between the edge effect the femoral stem and the micro-cavity is responsible for this behavior.

Fig.9 illustrates the variations of maximum equivalent stress as a function of the radial displacement of the micro-cavity in cement layer. The obtained results shown in this figure confirm those illustrated in Fig. 8. It can be noted that the presence of the micro-cavity has an effect on the change in the stress field at the two interfaces. Indeed, the maximal stress is obtained when the micro-cavity is located at the vicinity of cup/cement. Far from this interface, the maximum stress decreases progressively to reach its minimum value in the vicinity of second interface. Whatever the radial position of the micro-cavity, the cement is subjected to tensile stress. This can constitute a major risk of failure of cement or initiation of micro-crack.

Fig. 10 show the distribution of radial and angular stress around the micro-cavity, in the vicinity of the interface cup-cement and for $\theta = 40^\circ$. Regardless of the posi-

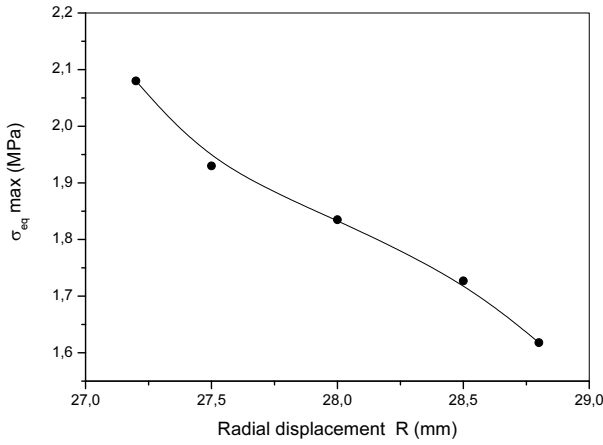


Fig. 9 $\sigma_{eq\ max}$ for different position R in cement

tion, the cement is completely compressed along both radial and angular directions.

The angular and radial stresses are highly localized in the central and extreme positions around the micro-cavity. It can be seen that the intensity of the radial stresses σ_r in different positions of the layer cement is higher than that angular stress σ_θ but their distributions are almost similar. By the low mechanical properties (compressive strength 80 MPa), the stress obtained around the micro-cavity do not present a risk of damage to the cement.

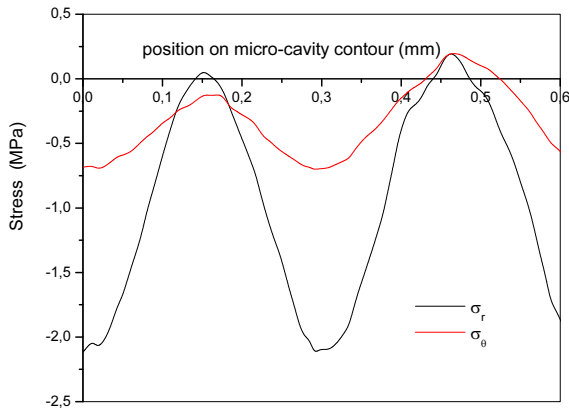


Fig. 10 Distribution of radial and angular stress around the micro-cavity, in the vicinity of the interface cup – cement

3.2. SIF for micro-crack emanating from micro-cavity

The SIFs behaviors along the micro-crack front were examined with respect to the gait cycle phases at different locations to study the micro-crack behavior in the cement layer. The micro-cavity is located at position $R = 27.2$ mm and $\theta = 40^\circ$. The SIFs were plotted versus the micro-crack front length in the different phases of the gait cycle. Figs. 11, 12, 13 represent the variation of stress intensity factors (K_I , K_{II} and K_{III}) of micro-crack emanating from micro-cavity for a gait cycle.

In mode I (Fig. 11), we note that the loading direction -12° leads to a stress intensity factor more important than for other orientations. On the other hand, whatever the loading orientation, the stress intensity factor increases along the micro-crack front and reaches its maximum value at its tip (position 1). This behavior is more marked in mode I.

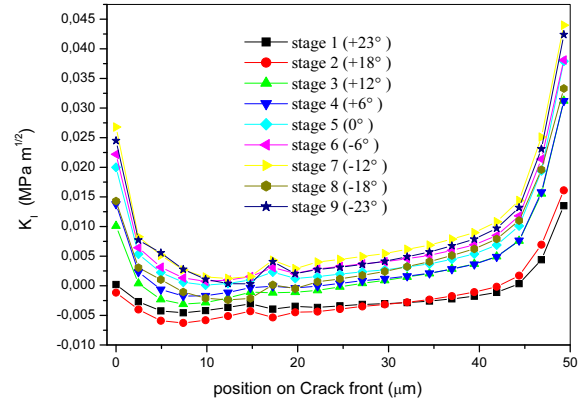


Fig. 11 Variation of K_I along de micro-crack front

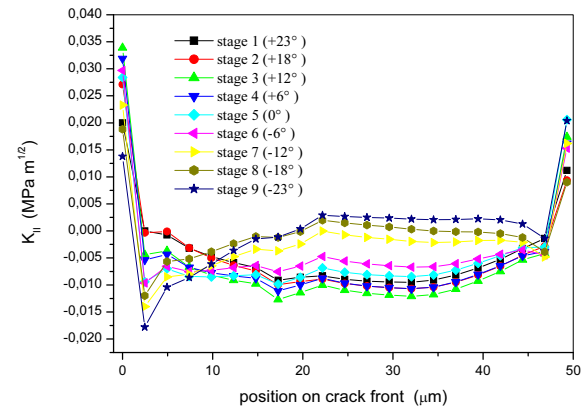


Fig. 12 Variation of K_{II} along de micro-crack front

The stress intensity factor in mode II (Fig. 12) varies weakly along the front; it reaches its maximum value at position 0 and then decreases to grow at the second tip (position 1). We note that regardless of the loading direction, the micro-crack propagation in mode II is stable and is characterized by a stress intensity factor almost null along the micro-crack front. In mode III (Fig. 13), the micro-crack does not present a risk of propagation because of the weak values of K_{III} along the micro-crack front.

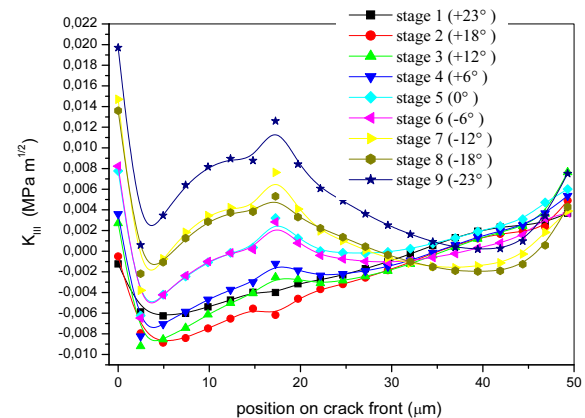


Fig. 13 Variation of K_{III} along de micro-crack front

Our results show that the most intense variations of the stress intensity factor are obtained in mode I (Fig. 14) for loading oriented at -12° . This orientation corresponds to the maximum load, reached during the gait cycle. In this case, the cement has a high risk of micro-crack propagation in mode I compared to other failure modes II and III.

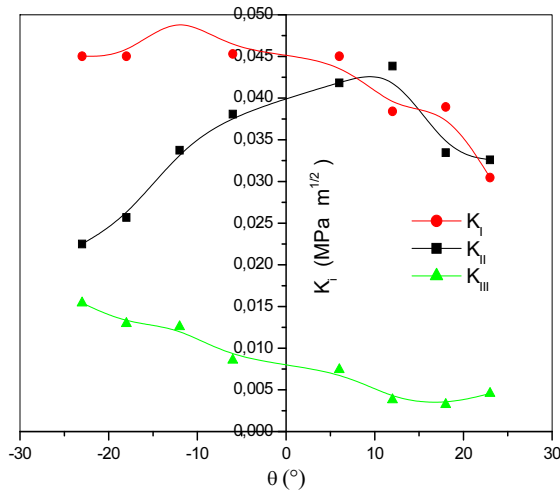


Fig. 14 Comparison of SIFs in mode I, II and III

4. Conclusion

This study was undertaken with an aim of analyzing the behavior of a micro-crack emanating from the micro cavity located in cement of reconstructed acetabulum by the calculation of the stress intensity factors along the micro-crack front under a gait cycle. The obtained results allow us to deduce the following conclusions:

1. The distribution of the stress around the micro-cavity in the cement layer is not homogeneous. The Von Mises stresses increase with angle θ , where they reach their maximum values at $\theta = 40^\circ$. From this orientation the intensity of equivalent stress decreases and reaches their minimum value at 90° . The cement around the micro-cavity is subjected to tensile loading. This can constitute a major risk for the micro-crack initiation emanating from the micro-cavity.

2. The extreme positions 0 and 90° generate almost the same distribution and the same level of stress. In his positions the cement is completely relaxed; the stresses are extremely low they do not constitute an immediate risk of damage of the cement.

3. The radial displacement results an almost uniform distribution of stresses with the highest values is located in close vicinity of interface cup / cement. These stresses reach their minimum value in the vicinity of the cement / cortical bone interface.

4. The intensity of the radial stresses in different positions of the layer cement is higher than that angular stress. The radial and angular stress obtained around the micro-cavity does not present a risk of damage to the cement.

5. The presence of the micro-cavity has an effect on the variation of the stress intensity factor. The SIFs in mode I, II and III depends on the positions of the micro-crack around the micro-cavity in the cement and the gait cycle. The stress intensity factor in mode I increase along the micro-crack front and reach its maximum value at position 1. The stress intensity factor in mode II varies weakly along the front and the micro-crack propagation in this mode is stable. In mode III, the micro-crack does not present a risk of propagation because of the weak values of K_{III} along the micro-crack front.

6. The most important variations of the stress intensity factor are obtained in mode I for loading oriented -

12° . This orientation corresponds to the maximum load, reached during the gait cycle. In this case, the cement has a high risk of micro-crack propagation in mode I compared to other failure modes II and III.

References

1. Dunne, N.J.; Orr, J.F.; Mushipe, M.T.; Eveleigh, R.J. 2003. The relationship between porosity and fatigue characteristics of bone cements, *Biomaterials* 24: 239-245. [http://dx.doi.org/10.1016/S0142-9612\(02\)00296-X](http://dx.doi.org/10.1016/S0142-9612(02)00296-X).
2. Jeffers, J.R.T.; Browne, M.; Roques, A.; Taylor, M. 2005. On the importance of considering porosity when simulating the fatigue of bone cement, *Journal of Biomechanical Engineering* 127: 563-570. <http://dx.doi.org/10.1115/1.1934182>.
3. Jeffers, J.R.T.; Browne M.; Lennon A.B.; Prendergast P.J.; Taylor, M. 2007. Cement mantle fatigue failure in total hip replacement, *Journal of Biomechanics* 40: 1525-1533. <http://dx.doi.org/10.1016/j.jbiomech.2006.07.029>.
4. Hoey, D.; Taylor, D. 2008. Fatigue in porous PMMA: the effect of stress concentrations, *International Journal of Fatigue* 30: 989-995. <http://dx.doi.org/10.1016/j.ijfatigue.2007.08.022>.
5. Hoey, D.; Taylor, D. 2009. Quantitative analysis of the effect of porosity on the fatigue strength of bone cement, *Acta Biomaterialia* 5: 719-726. <http://dx.doi.org/10.1016/j.actbio.2008.08.024>.
6. Cristofolini, L.; Minari, C.; Viceconti, M. 2000. A methodology and criterion for acrylic bone cement fatigue tests, *Fatigue and Fracture of Engineering Materials and Structures* 23: 953. <http://dx.doi.org/10.1046/j.1460-2695.2000.00327.x>.
7. McCormack, B.A.O.; Prendergast, P.J. 1999. Micro-damage accumulation in the cement layer of hip replacements under flexural loading, *Journal of Biomechanics* 32: 467-475. [http://dx.doi.org/10.1016/S0021-9290\(99\)00018-4](http://dx.doi.org/10.1016/S0021-9290(99)00018-4).
8. Murphy, B.P.; Prendergast, P.J. 2000. On the magnitude and variability of the fatigue strength of acrylic bone cement, *International Journal of Fatigue* 22: 855-864. [http://dx.doi.org/10.1016/S0142-1123\(00\)00055-4](http://dx.doi.org/10.1016/S0142-1123(00)00055-4).
9. Lewis, G.; Janna, S.; Bhattaram, A. 2005. Influence of the method of blending an antibiotic powder with an acrylic bone cement on physical, mechanical, and thermal properties of the cured cement, *Biomaterials* 26: 4317-4325. <http://dx.doi.org/10.1016/j.biomaterials.2004.11.003>.
10. Wixson, R.L.; Lautenschlager, E.P.; Novak, M.A. 1987. Vacuum mixing of acrylic bone cement, *The Journal of Arthroplasty* 2: 141-149. [http://dx.doi.org/10.1016/S0883-5403\(87\)80021-9](http://dx.doi.org/10.1016/S0883-5403(87)80021-9).
11. Alkire, M.; Dabezies, E.; Hastings, P. 1987. High vacuum as a method of reducing porosity of polymethylmethacrylate, *Orthopedics* 10: 1533-1539.
12. Ling, R.S.; Lee, A.J. 1998. Porosity reduction in acrylic cement is clinically irrelevant, *Clinical Orthopaedics*: 249-253. <http://dx.doi.org/10.1097/00003086-199810000-00026>.
13. Goldring, S.R.; Schiller, A.L.; Roelke, M.; Rourke,

- C.M.; O'Connor, D.O.; Harris, W.H. 1983. Formation of a synovial-like membrane at the bone cement interface, *J Bone J Surg*; A65: 575-84.
14. Jasty, M.; Malony, W.J.; Bragdon, C.R.; O'Connor, D.O.; Haire, T.; Harris, W.H. 1991. The initiation of failure in cemented femoral components of hip arthroplasties, *J Bone Joint Surg*; B73: 551-558.
 15. Ling, R.S.M.; Lee, J.C. 1998. Porosity reduction in acrylic cement is clinically irrelevant, *Clinical Orthopedics* 355: 249-253.
<http://dx.doi.org/10.1097/00003086-199810000-00026>.
 16. Benbarek, S.; Bachir Bouiadjra, B.; Mankour, A.; Acour, T.; Serier, B. 2009. Analysis of fracture behaviour of the cement mantle of reconstructed acetabulum, *Computational Materials Science* 44: 1291-1295.
<http://dx.doi.org/10.1016/j.commatsci.2008.08.024>.
 17. Ouinas, D.; Flliti, A.; Sahnoun, M.; Benbarek, S.; Taghezout, N. 2012. Fracture behavior of the cement mantle of reconstructed acetabulum in the presence of a microcrack emanating from a microvoid, *International Journal of Materials Engineering* 2(6): 90-104.
 18. Achour, T.; Tabeti, M.S.H.; Bouziane, M.M.; Benbarek, S.; Bachir Bouiadjra, B.; Mankour, A. 2010. Finite element analysis of interfacial crack behavior in cemented total hip arthroplasty, *Computational Materials Science* 47: 672-677.
<http://dx.doi.org/10.1016/j.commatsci.2009.10.007>.
 19. Flitti, A.; Ouinas, D.; Bouiadjra, B.B.; Benderdouche, N. 2010. Effect of the crack position in the cement mantle on the fracture behavior of the total hip prosthesis, *Comput MaterSci*. 49: 598-602.
<http://dx.doi.org/10.1016/j.commatsci.2010.05.056>.
 20. Serier, B.; Bachir Bouiadjra, B.; Benbarek, S.; Achour, T. 2009. Analysis of the effect of the forces during gait on the fracture behaviour in cement of reconstructed acetabulum, *Computational Materials Science* 46: 267-274.
<http://dx.doi.org/10.1016/j.commatsci.2009.03.003>.
 21. Bachir Bouiadjra, B.; Belarbi, A.; Benbarek, S.; Achour, T.; Serier, B. 2007. FE analysis of the behaviour of micro-cracks in the cement mantle of reconstructed acetabulum in the total hip prosthesis, *Computational Materials Science* 40: 485-491.
<http://dx.doi.org/10.1016/j.commatsci.2007.02.006>.
 22. Bouziane, M.M.; Bachir Bouiadjra, B.; Benbarek S.; Tabeti, M.S.H.; Achour, T. 2010. Finite element analysis of the behaviour of microvoids in the cement mantle of cemented hip stem: Static and dynamic analysis, *Materials and Design* 31: 545-550.
<http://dx.doi.org/10.1016/j.matdes.2009.07.016>.
 23. Benbarek, S.; Bachir Bouiadjra, B.; Achour, T.; Belhouari, M.; Serier, B. 2007. Finite element analysis of the behaviour of crack emanating from microvoid in cement of reconstructed acetabulum, *Materials Science and Engineering A* 457: 385-391.
<http://dx.doi.org/10.1016/j.msea.2006.12.087>.
 24. Tong, J.; Wong, K.Y. 2005. Mixed Mode Fracture in Reconstructed Acetabulum, Department of Mechanical and design Engineering, University of Portsmouth, Anglesea road, Portsmouth, PO1 3 DJ, UK.
 25. Nikolaus, P.Z.; Wong, C.K.Y.; Tong, J. 2007. Fatigue failure in the cement mantle of a simplified acetabular replacement model, *International Journal of Fatigue* 29: 1245-1252.
<http://dx.doi.org/10.1016/j.ijfatigue.2006.10.013>.
 26. Phillips, A. 2001. Finite Element Analysis of the Acetabulum after Impacting Grafting, The University of Edinburgh, School of Civil and Environmental Engineering, Crew Building, Kings Buildings, Edinburgh EH93JN.
 27. Christopher, L.P.; Kent, N.B.; Marcis, A.C.; Thomas, O.H. 2001. The effect of femoral prosthesis design on cement strain in cemented total hip arthroplasty, *Journal of Arthroplasty* 16(2): 216-224.
<http://dx.doi.org/10.1054/arth.2001.20537>.
 28. Schuller, H.M.; Dalstra, M.; Huiskes, R.; Marti, R.K. 1993. Total hip reconstruction in acetabular dysplasia: a finite element study, *J Bone Joint Surg [Br]* 75-B: 468-474.
 29. Saikko, V.; Paavolainen, P.; Kleimola, M.; Slati, P. 1992. A five-station hip joint simulator for wear rate studies, *Proc. Instn. Mech. Eng.* 206: 195-200.
http://dx.doi.org/10.1243/PIME_PROC_1992_206_291_02.
 30. Saikko, V. 1996. Three-axis hip joint simulator for wear and friction studies on total hip prostheses, *Proc. Instn. Mech. Eng.* 210: 175-185.
http://dx.doi.org/10.1243/PIME_PROC_1996_210_410_02.
 31. Saikko, V. 1998. A multidirectional motion pin-on-disk wear test method for prosthetic joint materials, *J. Biomed. Mater. Res.* 41(1): 58-64.
[http://dx.doi.org/10.1002/\(SICI\)1097-4636\(199807\)41:1<58::AID-JBM7>3.0.CO;2-P](http://dx.doi.org/10.1002/(SICI)1097-4636(199807)41:1<58::AID-JBM7>3.0.CO;2-P).
 32. Wu, J.S.S.; Hung, J.P.; Shu, C.S.; Chen, J.H. 2003. The computer simulation of wear behavior appearing in total hip prosthesis, *Computer Methods and Programs in Biomedicine* 70: 81-91.
[http://dx.doi.org/10.1016/S0169-2607\(01\)00199-7](http://dx.doi.org/10.1016/S0169-2607(01)00199-7).
 33. Oshkour, A.A.; Davoodi, M.M.; Abu Osman, N.A.; Yau, Y.H.; Tarlochan, F.; Wan Abas, W.A.B. 2013. Finite element analysis of circumferential crack behavior in cement-femoral prosthesis interface, *Materials and Design* 49: 96-102.
<http://dx.doi.org/10.1016/j.matdes.2013.01.037>.
 34. ABAQUS/CAE Ver 6.9.2007. User's Manual. Hibbit, Karlsson & Sorensen, Inc.

N. Bounoua, A. Belarbi, M. Belhouari,
B. Bachir Bouiadjra

MIKROPLYŠIO ATSIRANDANČIO DĖL
MIKROTUŠTUMŲ REKONSTRUOTOS GŪŽDUOBĖS
CEMENTE ĮTEMPIŲ INTENSYVUMO
KOEFIČIANTAI

R e z i u m ė

Cementas yra pagrindinis elementas apsaugantis kaulo taurę. Jo pagrindinis vaidmuo užtikrinti gerą sukibimą ir apkrovos perdavimą kaului. Cemento mechaninės savybės yra labai menkos. Veikiant mechaninei apkrovai cementas privalo priešintis mikroplyšio atsiradimui ir sklidimui, kuris iššaukia protezo ardymą ir, dėl šios priežasties, protezo atplėšimą. Šioje studijoje naudojamas 3D baigtinių elementų metodas įtempių pasiskirstymo apie rekonstruotos gūžaduobės mikrotuštumas cemente analizei. Išryškinta mikrodefekto padėties įtaka įtempių pasiskirsty-

mui. Taip pat analizuojamas mikroplyšio sklidimas iš mikrotuš-
tumos skaičiuojant įtempių intensyvumo koeficientą mikroplyšio
viršūnėje žmogui žingsniuojant.

N. Bounoua, A. Belarbi, M. Belhouari,
B. Bachir Bouiadjra

STRESS INTENSITY FACTORS FOR MICRO-CRACK
EMANATING FROM MICRO-CAVITY IN CEMENT
OF RECONSTRUCTED ACETABULUM

S u m m a r y

Cement is an essential element for securing the
cup to the bone. Its main role is to ensure good adhesion
and to ensure the load transfer to the bone. The mechanical
properties of cement are very low. Under the effect of the

mechanical loading, cement must be able to resist the initia-
tion and propagation of micro-crack being able to lead to
its ruin and consequently the unsealing of the prosthesis. In
this study, the three-dimensional finite element method is
used to analyze the stress distribution around micro cavi-
ties in the cement of reconstructed acetabulum. The effect
of the position of the micro defect on the stress distribution
is also highlighted. On the other hand to analyze the behav-
ior of micro-crack emanating from micro-cavity by com-
puting the stress intensity factor at the micro-crack tip un-
der a gait cycle.

Keywords: Cement; Micro-cavity; Micro-crack; Stress
intensity factors; Finite element method.

Received July 12, 2014

Accepted November 17, 2014